Digital Manufacturing for Electrically Functional Satlet Structures

Paul I. Deffenbaugh[1], Mike Newton[2], and Kenneth H. Church[1].

[1] Sciperio, Inc.
Orlando, FL, 32826, USA

[2] Newton Cyberfacturing, Inc.
Orlando, FL, 32826, USA

Email: pdeffenbaugh@sciperio.com, mike@newtoncyberfacturing.com, khc@sciperio.com

Abstract
3D printing structures is natural for the layer by layer approach. Using a single type of material and building complex structures is not optimized but it is mature. This digital approach to manufacturing has the advantages of lighter structures that maintain strength and can also address the emerging custom market. While these are important contributions, adding electrically functional characteristics to the structures will open new opportunities for next generation products. In the case of the presented materials, the target application is small satellite or Satlets. Adding electronics to 3D structures is not optimized or mature and therefore studying this will be important to understand the potential and the obstacles that must be addressed. Utilizing the combination of 3D printing and printed electronics, we printed a number of device demonstrations the show it is feasible to make diverse shapes with functional electronics. Demonstrations included 3D printed multilayer ceramic Ethernet harness, 3D printed plastic RF controlled impedance interconnect and USB harness and finally 3D printed connectors. Data will be presented on mechanical integrity of printed structures and electrical performance.

Key words
Direct Digital Manufacturing, Additive Manufacturing, 3D Printing, Satellites, Printed Electronics.

I. Introduction

3D printing today consists primarily of a single material type only (fused molten plastic, sintered powder, cured resin, etc.). Here is shown a true heterogeneous mixture of materials that will be processed in accordance with individual material requirements. A new generation of 3D composites will emerge from these efforts with diverse and disparate materials that have been optimized to account for thermal mismatch using a gradient approach and newly engineered micro- and nano-structures. This includes: 3D printed mixed metals, polymers, ceramics, plastics and semiconductors. Several specific examples are shown, a 3D printed wiring harness, connectors and a 3D printed satlet structure. A satlet is a micro satellite with approximate dimensions of 10 x 10 x 10 cm which when connected with other satlets can perform some larger task. A new integrated mechanical/electrical connector strategy is demonstrated as well.

II. Material Selection

Materials typically serve a specific function in building devices. Generally they either serve a mechanical (structural) function or an electrical (conductive) function so the need to build using a multi-material process for a multifunctional systems is what drives material selection decisions. How the harness is integrated in a satlet influenced these decisions. The 3D printed process is also a parameter that is used in making material selections for supporting the technology demonstrators. For high temperature processing as is need for the aluminum sunshade implementation drove the decision to look at ceramic materials and high temperature silver conductors. Experience in process low temperature co-fired ceramics is applied here. These materials fire in a range from 590 °C to 900 °C. They have been space and DoD qualified for Multichip module fabrication. In this study these materials are able to be printed using the nScrypt direct print process since it is converted for a tape cast material to a printable paste.

The next configuration is to use thermoplastics as a basis for structural printing such as ULTEM. This is coupled with materials developed by industry for low temperature printed electronics. This integration of conductive materials like CB028 is developed by DuPont and has a curing temperature compatible to integrating into nFD printing of thermoplastics. nFD is a high resolution printing which is a temperature extrusion process similar to FDM.

Additionally, adjacent industries are surveyed for material availability which led to the desire to move into a pellet format versus the traditional filament format of thermoplastic materials. Pellets are the plastic raw material used by the injection mold industry. Materials available in pellet form is virtually limitless whereas materials available in filament form is limited to a handful. Furthermore, filaments are fabricated from the pellets which increases material cost from 10 to 20X. Hopper feed process enables the use of a much wider material selection and significant reduction in cost.

III. 3D Printed Wiring Harness

The ultimate goal of 3D printing by anyone involved in the industry is to be able to build final products. The goal of this effort is to target a harness as a means to demonstrate the feasibility of printing a subcomponent of a typical satellite system. The ability to 3D print multi-materials represents a digital manufacturing process that represents "System Integration" of materials/functions. As outlined in the initial harness design task, target demonstrators are identified.

Several test coupons are fabricated to support two potential implementations of an Ethernet or USB harness. The first is to fabricating an Ethernet harness directly on aluminum to demonstrate implanting on the existing sun shade design. 3D conformally printing of conductors and dielectrics needed to be understood as a result a fully functional ceramic on aluminum is successfully fabricated and tested. The second implementation is fabricating full 3D printing of thermoplastics and integrated conductors is studied and successfully implemented.

A 3D fabricated multi-material harness that integrates both mechanical and electrical functionality incorporating the following interconnects is developed. The lose strands of wires in Satlets take space, require room to assemble and have connector joints that fail. Printed Circuit Structures (PCS) reduce complexity and increase reliability. The following requirements for a satlet wiring harness are identified:

1. Power bus lines
2. USB differential pair
3. Ethernet differential pair
4. RF 50 ohm controlled impedance lines

A. Power bus lines

The satlet power sources are reconfigurable lithium ion or lithium polymer 3-4 VDC batteries and are rated at up to 4 A current. One identified demonstrator is the fabrication of a pressure vessel which contains the batteries. Based on material selection the pressure vessel is modeled for 200 psi with a 0.5 liter internal volume that accommodates 4 lithium ion batteries (18650 w/ tabs). The model includes an integral through-wall power buss that handles the amperage identified for the power load. The 3D printed wiring dimensions on the top of the sphere are 20 mm long. Based on the 4 amp current requirement the printed line width is chosen to be 10 mm width x 0.040 mm thick to reduce unwanted excessive heat transfer and power loss.

Figure 1 Pressurized battery power source

B. CAT5

Two specific protocols, Ethernet and USB, are focused on for the ability for potential plug and play of modular satlets and subcomponents within each satlet. A camera incorporated into a sun shade structure (12" diameter, 18" length) requires either USB or Ethernet connectivity through the structure. This is the basis for two options in fabricating a 3D printed harness. The first focused on a high temperature materials (9500 dielectric powder mixture printed on aluminum substrate) that could be 3D conformally printed onto the existing aluminum sunshade. The second is for a lower temperature ULTEM harness that could be integrated to a 3D printed ULTEM sunshade. The transmission line type is differential microstrip.

Performance is verified by connecting Ethernet cable and transferring 1 GB files via 100 Mbps 100-baseT.

Figure 2 3D printed Ethernet

Dimensions are determined by running an Ansys Q2D simulation of the cross section of the printed conductors (differential microstrip) on printed and sintered ceramic on the aluminum substrate. Impedance is designed to the 100 ohm Ethernet standard.

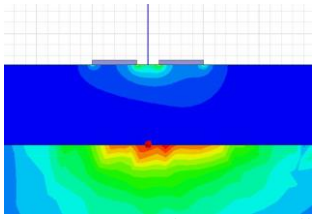

Figure 3 Ansys Q2D simulation of 3D printed differential microstrip for Ethernet

Full 3D printing is demonstrated by printing conformally around a bent piece of aluminum. Surface tracking using laser scanning is used and performance is verified.

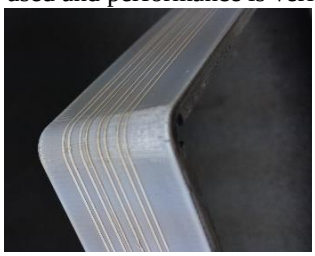

Figure 4 3D printed Ethernet 3D bend

A twisted pair is demonstrated as well by printing the lower lines first, then an additional dielectric coat, followed by the upper lines last.

Figure 5 3D printed twisted pair

Figure 6 3D printed twisted pair connection to RJ-45 jack

C. *Stripline*

In order to facilitate radio transmission from a satlet structure, antennas are needed and 3D printed antennas are already a reality. A requirement for wiring harnesses is controlled impedance (50 Ω) RF transmission lines. A stripline structure is designed and tested. Dielectric constant is around 2.6 and loss tangent is around 0.007-0.014. Conductivity is measured to be $4.6 \cdot 10^6$ S/m at DC and $2.5 \cdot 10^6$ S/m at 5 GHz probably due the skin effect, surface roughness, 3D printing effects as well as current flow through the polymer thick film composition of silver flakes.

In order to showcase the reality of direct digital manufacturing, a model of the structure and test probes is drawn in CAD and then 3D printed as shown in the following two images.

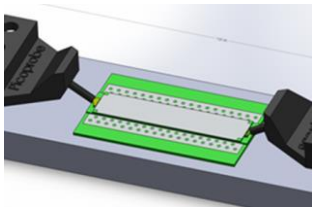

Figure 7 Digital rendering of 3D printable stripline

Figure 8 Actual fully 3D printed stripline test setup

The loss as measured using a VNA at a wide range of frequencies is shown below. Data matches closely with theory. Loss in transmission lines typically follows a linear plus square-root of frequency trend with contributions from dielectric loss tangent and conductor conductivity. Performance appears good up to about 7 GHz. This is likely due to the width of the top side ground and there is room for improvement in the upper frequency limit of this structure using existing 3D printing resolution.

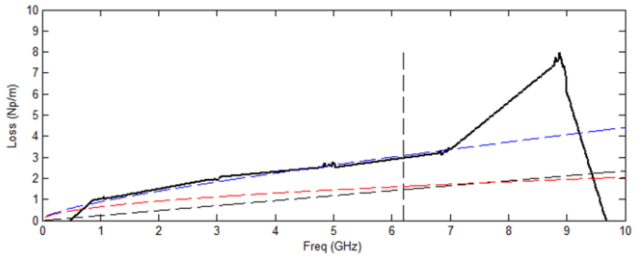

Figure 9 Loss vs. frequency in stripline

Black: total loss, measured
Blue: total loss, curve-fit
Dash/red: conductor loss
Dash/black: dielectric loss

IV. 3D Printed Connectors

In addition to an interconnect harness, methods for removable connections are required. Test structures are fabricated including battery connections, Ethernet, USB, and universal magnetic connections.

A. *Power connections*

Large area, high current (4 amp) connections are provided straight through the structure of the sphere while maintaining

a good seal against leakage. Landing-like connectors allow regular wires to be connected for testing and evaluation of the sphere or a 3D printable connector could be attached.

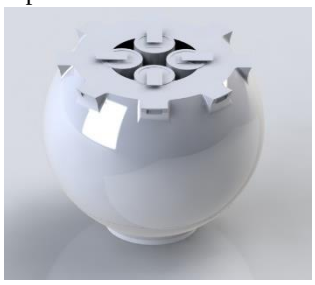

Figure 10 Sphere with 4 amp charging connections

B. Ethernet

Referring to the figure below, the prongs fit into the grooves on the 3D printed adapter, making a press fit with the printed conductive lines and transitioning to the 3D printed ceramic differential microstrip line.

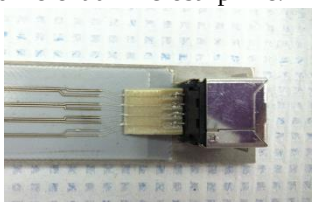

Figure 11 RJ-45 Ethernet port with adapter

C. USB connection

A USB connection is designed and fabricated which allows standard cables to be plugged and unplugged from 3D printed subsystems.

A fully 3D printed lighted LED dongle demonstrates the mechanics of the connection functioning.

Figure 12 Fully 3D printed lighted LED dongle

The connection is tested using a USB camera and full speed throughput is verified.

Figure 13 USB camera connection

D. Universal Magnetic Connectors

The satlet concept is that assembly can occur in space between modules. A 3D printable magnetic snap design is proposed. A test structure is fabricated that simulates a plug and play satlet with inter-module interconnect capability. Several interim test coupons and stand alone "magnetic connectors" are fabricated and lessons learned integrated into the satlet power hub module.

The magnetic connections are constructed in such a way that the conductive line (1 mm wide) on the dielectric is routed to the edge of the surface where it meets a larger (3 mm), contact surface which is printed onto the vertical surface using an angle printing pump. Extra material is deposited on this contact surface so as to facilitate a reliable connection.

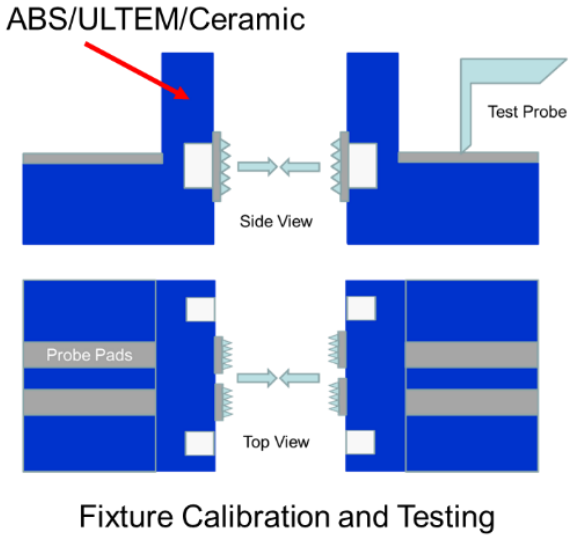

Figure 14 Magnetic interconnect diagram

Magnets are installed during the printing process using pick and place and are then totally encased in printed dielectric.

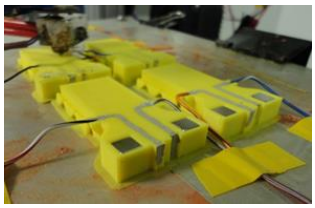

Figure 15 Magnetic connection 3D printing

Pick and place magnet installation during printing

The pull force is measured and verified. Connection resistance is verified over 20 cycles and during pull force testing.

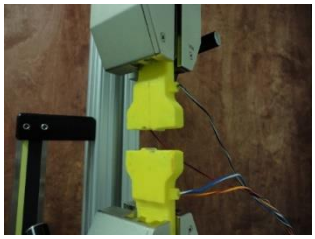

Figure 16 Pull force testing of magnets

In order to ensure long-term reliability of permanent satlet connections the option of laser-welding each connection is demonstrated and proven using simultaneous pull testing and conductivity measurement.

V. Satlet System

As a demonstrator, a wireless camera system is broken into subparts, each part as a satlet. When all of the satlets are interconnected (in space) the intended function commences. Additional functionality could be easily added or subtracted or failed components can be easily repaired even in space. A hexagonal architecture is chosen that allows function-satlets to be connected in any configuration on each if the six sides. Power is obtained by solar satlet modules which attach vertically. Each satlet has a different function: solar power, camera sensor, battery power, and RF transmitter.

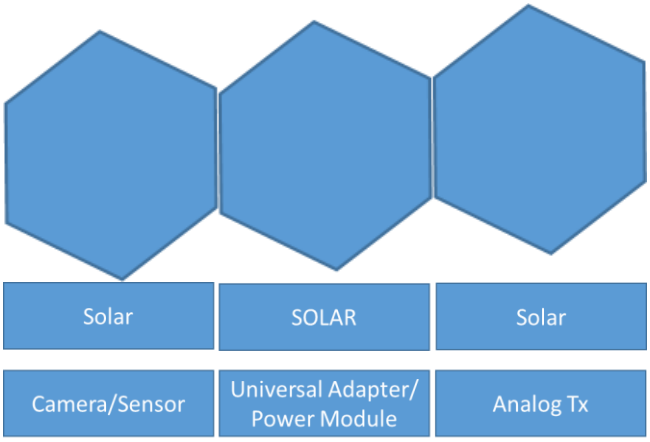

Figure 17 Satlet system block diagram (top view and side views)

N52 grade magnets are used which provide greater than 4.5 kg of attraction each to allow for adequate compression force on conductive connectors and to ensure no separation during operation. Four each are used on horizontal connections. Two each are used on vertical connections.

The horizontal electrical interconnects and magnetic joiners are shown below. +3.7 VDC bus voltage is present on the top connection, 0V/GND is connected in the center, and the 1V analog composite video signal is shared at the bottom terminal.

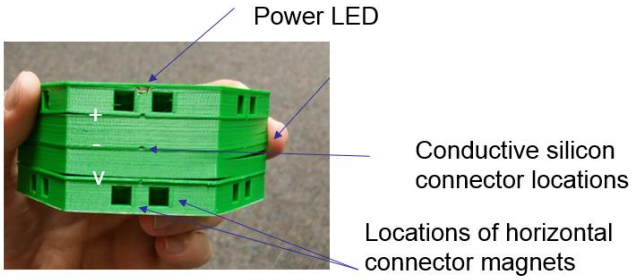

Figure 18 Open-side view of magnetic interconnects

The vertical electrical interconnects for solar power connections are shown below. Polarity is enforced by the magnetic poles. Magnets are embedded within the structure and printed over with additional plastic.

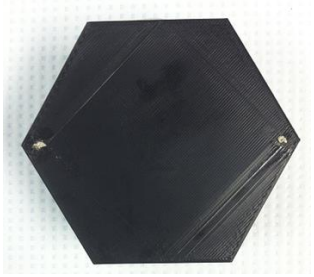

Figure 19 Vertical interconnects

A. Solar power

Up to one solar power satlet can be magnetically joined to each functional satlet and power is shared. Each solar satlet incorporates a 6V polycrystalline solar cell and a 3.7V solar charge controller which optimizes the current from each solar cell individually and charges battery power satlet or satlets via the 3.7V bus voltage lines. The vertical magnetic and electrical connection is demonstrated.

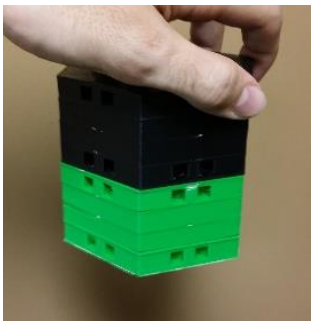

Figure 20 Vertical interconnect, solar satlet connected to camera satlet

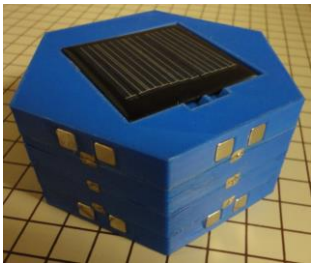

Figure 21 Solar satlet

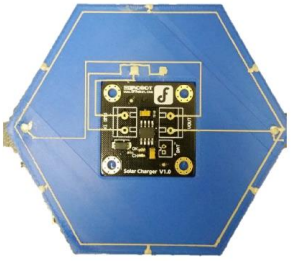

Figure 22 Solar power internal charge controller

B. *Analog Camera Satlet*

A 3.7V CMOS imager sensor with integrated composite video output is chosen and 3D printed into the satlet structure. Provisions are made for a 12 mm adjustable camera lens which points downwards (in the opposite direction from the solar power connections). A power on LED and resistor are provided in the integrated structure for monitoring.

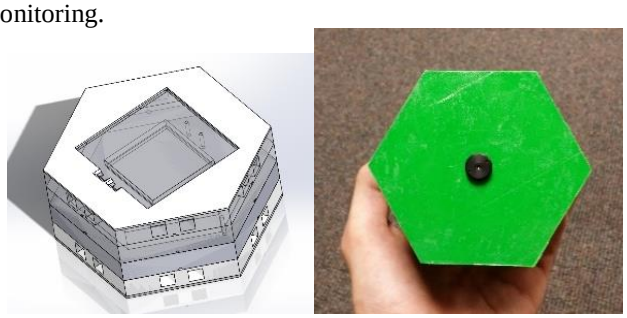

Figure 23 Camera satlet

C. *Battery Power*

A single-cell 3.7V 800 mAh lithium polymer battery is used for its low profile and compact energy density. A form-fitted cavity allows installation of the battery during printing. In the final design, power is routed directly from the battery tabs to printed lines in the satlet and through vertical interconnects (vias) to various levels of the satlet and to each of the six faces connectors.

Figure 24 Battery satlet

D. *RF transmitter*

A 2.4 GHz RF video transmitter is incorporated into the satlet system which accepts the analog video signal from the camera sensor and transmits it to a receiver. The transmitter is integrated within the satlet and a printed wire dipole for 2.4 GHz radiates the signal through the plastic structure.

Figure 25 RF transmitter satlet

Acknowledgements

DARPA contract “3D Printed Wire Harness Connectors for Satlets” Sciperio, Inc.

Additional thanks to Nick LaGana, Sam LeBlanc, Casey Perkowski, Harvey Tsang, and Andre Yanez for their contributions to this work.

References

[1] R. A. Ramirez, E. A. Rojas-Nastrucci, and T. M. Weller, "3D tag with improved read range for UHF RFID applications using Additive Manufacturing," in *Wireless and Microwave Technology Conference (WAMICON), 2015 IEEE 16th Annual*, 2015, pp. 1-4.

[2] Paul Deffenbaugh, "3D Printed Electromagnetic Transmission and Electronic Structures Fabricated on a Single Platform using Advanced Process Integration Techniques," Ph.D. dissertation, Elect. & Comput. Eng., UTEP, El Paso, TX, 2014.

[3] MIL STD 883. http://www.dscc.dla.mil/downloads/milspec/docs/mil-std-883/std883.pdf

[4] NASA Electronic Parts and Packaging Hermeticity. http://nepp.nasa.gov/workshops/etw2013/talks/Tue_June11_2013/1630_McManus_Pressnell_Hermeticity%20Leak%20Testing.pdf

[5] NovaWurks' Hyper-Integrated Satlet – HISat Hyper integrated satellite. http://www.youtube.com/watch?v=v0kYSmus_PI

[6] Paul I. Deffenbaugh, Thomas M. Weller, Kenneth H. Church, “Fabrication and Microwave Characterization of 3D Printed Transmission Lines,” submitted for publication.

[7] Paul I. Deffenbaugh, Josh Goldfarb, Xudong Chen, Kenneth H. Church, “Fully 3D Printed 2.4 GHz Bluetooth/Wi-Fi Antenna,” IMAPS, 46th International Symposium on Microelectronics, Orlando, Florida, September 30 – October 3, 2013.

[8] C. D. Gutierrez, R. Salas, G. Hernandez, D. Muse, R. Olivas, E. MacDonald, M. Irwin, M. Newton, K. Church, B. Zufelt, “CubeSat Fabrication Through Additive Manufacturing and Micro-Dispensing,” IMAPS 2011.

[9] Church, K.; MacDonald, E.; Clark, P.; Taylor, R.; Paul, D.; Stone, K.; Wilhelm, M.; Medina, F.; Lyke, J.; Wicker, R., "Printed electronic processes for flexible hybrid circuits and antennas," Flexible Electronics & Displays Conference and Exhibition, 2009. , vol., no., pp.1,7, 2-5 Feb. 2009

[10] Kenneth H. Church, Xudong Chen, Joshua M. Goldfarb, Casey W. Perkowski, Samuel LeBlanc, “Advanced Printing for Microelectronic Packaging,” submitted for publication in IPC APEX Expo 2014, Las Vegas, Nevada, December 12, 2013.